TOXICOLOGICAL SCIENCES **110(1)**, 191–203 (2009)
doi:10.1093/toxsci/kfp051
Advance Access publication March 6, 2009

Pulmonary Nanoparticle Exposure Disrupts Systemic Microvascular Nitric Oxide Signaling

Timothy R. Nurkiewicz,*,†,‡,[1] Dale W. Porter,†,§ Ann F. Hubbs,§ Samuel Stone,§ Bean T. Chen,§ David G. Frazer,†,§ Matthew A. Boegehold,*,† and Vincent Castranova§

**Center for Cardiovascular and Respiratory Sciences, West Virginia University School of Medicine, Morgantown, West Virginia 26506; †Department of Physiology and Pharmacology, West Virginia University School of Medicine, Morgantown, West Virginia 26506; ‡Department of Neurobiology and Anatomy, West Virginia University School of Medicine, Morgantown, West Virginia 26506; and §Pathology and Physiology Research Branch, Health Effects Laboratory Division, National Institute for Occupational Safety and Health, Morgantown, West Virginia 26506*

Received January 19, 2009; accepted March 2, 2009

We have shown that pulmonary nanoparticle exposure impairs endothelium dependent dilation in systemic arterioles. However, the mechanism(s) through which this effect occurs is/are unclear. The purpose of this study was to identify alterations in the production of reactive species and endogenous nitric oxide (NO) after nanoparticle exposure, and determine the relative contribution of hemoproteins and oxidative enzymes in this process. Sprague-Dawley rats were exposed to fine TiO_2 (primary particle diameter ~1 μm) and TiO_2 nanoparticles (primary particle diameter ~21 nm) via aerosol inhalation at depositions of 4–90 μg per rat. As in previous intravital experiments in the spinotrapezius muscle, dose-dependent arteriolar dilations were produced by intraluminal infusions of the calcium ionophore A23187. Nanoparticle exposure robustly attenuated these endothelium-dependent responses. However, this attenuation was not due to altered microvascular smooth muscle NO sensitivity because nanoparticle exposure did not alter arteriolar dilations in response to local sodium nitroprusside iontophoresis. Nanoparticle exposure significantly increased microvascular oxidative stress by ~60%, and also elevated nitrosative stress fourfold. These reactive stresses coincided with a decreased NO production in a particle deposition dose-dependent manner. Radical scavenging, or inhibition of either myeloperoxidase or nicotinamide adenine dinucleotide phosphate oxidase (reduced) oxidase partially restored NO production as well as normal microvascular function. These results indicate that in conjunction with microvascular dysfunction, nanoparticle exposure also decreases NO bioavailability through at least two functionally distinct mechanisms that may mutually increase local reactive species.

Key Words: **systemic microcirculation; nitric oxide; nanoparticle; inhalation; arteriole; endothelium.**

The relationship between ambient particulate matter (PM) exposure and cardiovascular morbidity and mortality has been consistently reported by epidemiological studies for more than a decade (Dockery *et al.*, 1993). Adverse cardiovascular outcomes were initially associated with general or ambient PM; later an obvious need developed to identify specific component(s) of particle pollution responsible for untoward health effects. As a result of this, cardiovascular consequences of pulmonary exposure to fine PM (ambient particles with a mean aerodynamic diameter of 0.1–2.5 μm) or ultrafine PM (ambient particles with a mean aerodynamic diameter less than 100 nm) are now well known. Such consequences include (but are not limited to): myocardial infarction (Peters *et al.*, 2001), augmented ischemia-reperfusion injury (Cozzi *et al.*, 2006), altered vascular reactivity (Nurkiewicz *et al.*, 2004), arrhythmias (Wellenius *et al.*, 2002), and altered heart rate variability (Godleski *et al.*, 2000). Despite a fundamentally good understanding of the ramifications of PM exposure on cardiovascular health, the underlying mechanisms responsible for such health effects remain very poorly understood. Furthermore, during the development of the PM-health effects knowledge base, nanotechnology rapidly evolved to potentially impact most every sector of modern society. Because of this rapid evolution and the considerably diverse nature of nanoparticles (engineered particles with one dimension less than 100 nm), comparatively few studies have documented the potential health effects of nanoparticle exposure, let alone characterize its mechanistic pathways.

We have previously shown that pulmonary exposure to fine PM produces systemic microvascular dysfunction (Nurkiewicz *et al.*, 2004, 2006). The relative intensity of this dysfunction was not dependent upon the pulmonary toxicity of the PM because combustion-derived particles (residual oil fly ash) and similarly sized TiO_2 particles caused equivalent levels of dysfunction. Therefore, TiO_2 particles are used as environmental particle surrogates in experiments where specific elemental toxicity is undesirable. Although the pulmonary

[1] To whom correspondence should be addressed at Center for Cardiovascular and Respiratory Sciences, 1 Medical Center Drive, Robert C. Byrd Health Sciences Center, West Virginia University, Morgantown, WV 26506-9105. Fax: (304) 293-5513. E-mail: tnurkiewicz@hsc.wvu.edu.

toxicity of a given particle does not appear to dictate the peripheral effect, we have recently shown that compared with fine TiO_2, inhalation of TiO_2 nanoparticles does result in a profoundly greater level of microvascular dysfunction on an equal mass burden basis (Nurkiewicz *et al*., 2008). Although this dysfunction was shown to be localized almost entirely to the endothelium, further elucidation of mechanism(s) mediating particle-induced microvascular dysfunction is necessary.

Nitric oxide (NO) is perhaps the body's most ubiquitous second messenger, and it plays a fundamental role in numerous vascular functions such as endothelium-dependent dilation (Persson *et al*., 1990), angiogenesis (Matsunaga *et al*., 2002), and leukocyte adhesion (Nabah *et al*., 2005). Alterations in NO bioavailability after PM exposure have been implicated in the rat mesenteric vein (Knuckles *et al*., 2008), aorta (Sun *et al*., 2008), and skeletal muscle arterioles (Nurkiewicz *et al*., 2004). This alteration is thought to be due to the uncoupling of endothelial nitric oxide synthase (eNOS). In this state, eNOS produces reactive oxygen species (ROS) rather than NO. In the studies by Knuckles *et al*. (2008) and Sun *et al*. (2008), evidence of eNOS uncoupling included a lack of vascular responsiveness to competitive eNOS inhibitors and decreased endogenous tetrahydrobiopterin (BH_4) levels after particle exposure, respectively. Although not exclusively limited to eNOS uncoupling, an increased production of ROS in various vascular preparations has also been reported to follow particle exposure. Similarly, the accumulation of reactive nitrogen species (RNS) such as peroxynitrite in the systemic microvasculature may also follow particle exposure, but no study to date has explored such a possibility. This increase in local reactive species could potentially consume NO via redox reactions (Wilcox, 2003). However, a direct relationship between ROS or RNS and an NO deficit has not been established, largely because of the considerable difficulty associated with making direct NO measurements. Because NO bioavailability is not identical in all tissues, it is important to appreciate that the relative contribution of NO to a given biologic function in one tissue is not implicitly the same in another. More specifically, it is unlikely that the activity that NO contributes to in one tissue will be the same in another; and it is reasonable to assume that the amount of NO produced in these cases is not identical.

Because numerous reports have identified alterations in human cardiovascular function after PM exposure, most notably arterial pressure (Urch *et al*., 2005), vascular reactivity (Peretz *et al*., 2008; Tornqvist *et al*., 2007) and flow responsiveness (Rundell *et al*., 2007); it is critical to identify the status of NO bioavailability in the microcirculation under these conditions. This is largely because it is at this level of the circulation that vascular resistance is actively generated (Zweifach, 1991) and the influence of NO is most obvious (Bohlen and Lash, 1996). Furthermore, the effect of pulmonary nanoparticle exposure on endogenous NO production is completely unknown. Therefore, the objectives of this study were to (1) directly measure microvascular NO production, (2) determine the effect of nanoparticle exposure NO production, and (3) elucidate mechanisms that may alter endogenous NO bioavailability.

METHODS

Experimental animals. Specific pathogen free male Sprague-Dawley [Hla:(SD)CVF] rats (6–7 weeks old) were purchased from Hilltop Laboratories (Scottdale, PA) and housed in an Association for Assessment and Accreditation of Laboratory Animal Care approved animal facility at the National Institute for Occupational Safety and Health. Rats were housed in laminar flow cages under controlled temperature and humidity conditions and a 12-h light/12-h dark cycle. Food and water were provided *ad libitum*. Rats were acclimated for 5 days before use and certified free of endogenous viral pathogens, parasites, mycoplasms, *Helicobacter*, and CAR bacillus. To ensure that all methods were performed humanely and with regard for alleviation of suffering, all experimental procedures were approved by the Animal Care and Use Committees of the National Institute for Occupational Safety and Health, and West Virginia University.

Inhalation exposure. The inhalation exposure system used for particle exposures in the current experiments has been previously described (Nurkiewicz *et al*., 2008). Briefly, the system contains a fluidized-bed powder generator, an animal chamber, and assorted aerosol monitoring and control devices that are collectively capable of generating fine or nanoparticle aerosols. Fine and nano-TiO_2 powders were obtained from Sigma-Aldrich (titanium (IV) oxide, 224227, St Louis, MO) and DeGussa (Aeroxide TiO_2, P25, Parsippany, NJ), respectively. The fine TiO_2 powder is reported by the vendor to be ~99% rutile, with a primary particle size < 5 μm. The nano-TiO_2 powder is reported by the vendor to be 80% anatase, and 20% rutile, with a primary particle size of 21 nm. These proportions of anatase and rutile TiO_2 have been independently verified (Hurum *et al*., 2003; Stone and Davis, 1998; Vasiliev *et al*., 2008). Prior to aerosol generation, the dry, fine TiO_2 and nano-TiO_2 particles had BET surface areas (Brunauer *et al*., 1938) of 2.34 and 48.08 m^2/g, respectively (Sager *et al*., 2008). The mass median aerodynamic diameter (MMAD) of the aerosols were 402 nm for the fine TiO_2 (with a geometric standard deviation, GSD of 2.4), and 138 nm for the nano-TiO_2 (Nurkiewicz *et al*., 2008). The use of MMAD to characterize nanoparticle aerosols can be problematic in that a relatively small number of large agglomerates can disproportionately skew the sample; thus, rendering the measurement nonrepresentative of the total particle size distribution. Therefore, the use of count mode diameter (CMD) is better suited to characterize our aerosols; and in our studies, fine TiO_2 aerosols had a CMD of 710 nm and the nano-TiO_2 aerosols had a CMD of 100 nm (Nurkiewicz *et al*., 2008). Rats were housed in the exposure chamber for 240–720 min at aerosol concentrations of 1.5–16 mg/m^3 (Nurkiewicz *et al*., 2008). Time and aerosol concentration were manipulated to produce five different doses for each particle type, and produced actual lung burdens of 4–90 μg which were previously measured in ashed lung tissue (Nurkiewicz *et al*., 2008). The entire aerosol/exposure profile and particle depositions for each group can be found in Nurkiewicz *et al*. (2008). For the purpose of consistency between studies, these lung burdens were used again in the current series of experiments. The EC_{50} for each particle type was defined as the lung burden that produced ~50% impairment of microvascular reactivity. For the fine TiO_2 group, the EC_{50} was 67 μg, and was produced by a 300-min exposure to an aerosol concentration of 16 mg/m^3. For the nano-TiO_2 group, the EC_{50} was 10 μg, and was produced by a 240-min exposure to an aerosol concentration of 6 mg/m^3.

Intravital microscopy. At 24-h postexposure, rats were anesthetized with sodium thiopental (Pentothal, 100 mg/kg, i.p.) and placed on a heating pad to maintain a 37°C rectal temperature. The trachea was intubated to ensure a patent airway, and the right carotid artery was cannulated to measure arterial pressure. The right spinotrapezius muscle was then exteriorized for microscopic observation, leaving its innervation and all feed vessels intact. After exteriorization, the muscle was gently secured over an optical pedestal at its

in situ length. The muscle was next enclosed in a tissue bath for transillumination and observation. Throughout the surgery and subsequent experimental period, the muscle was continuously superfused with an electrolyte solution (119mM NaCl, 25mM $NaHCO_3$, 6mM KCl, and 3.6mM $CaCl_2$), warmed to 35°C, and equilibrated with 95% N_2–5% CO_2 (pH = 7.35–7.40). Superfusate flow rate was maintained at 4–6 ml/min to minimize equilibration with atmospheric oxygen (Boegehold and Bohlen, 1988).

The animal preparation was then transferred to the stage of an intravital microscope coupled to a CCD video camera. Observations were made with a 20× water immersion objective (final video image magnification = 1460×). One to three microvessels were studied per rat. Video images were displayed on a high-resolution color video monitor and videotaped for off-line analysis. During videotape replay, arteriolar inner diameters were measured with a video caliper (Cardiovascular Research Institute, Texas A&M University).

NO measurement. The left and right spinotrapezius muscles from the same animal were excised and placed in Ca^{2+}-free Dulbecco's phosphate-buffered saline (PBS). The excised muscles were pinned out on a Sylgard coated Petri dish and microvessels were dissected from the tissue at 4°C. The microvessels were lightly homogenized after collection and then briefly centrifuged to form a loose pellet. The pellet was then placed into a four-port, water jacketed (34°C), biosensing chamber (World Precision Instruments, Inc, Sarasota, FL) that contained 2 ml of Dulbecco's PBS with Ca^{2+} (3.6mM), L-arginine (0.2mM), and tetrahydrobiopterin (BH_4, 4μM). Two of the chamber ports contained ISO-NOP NO sensors (World Precision Instruments, Inc., Sarasota, FL), the third contained a temperature probe, and the forth was left open to add reagents to the chamber via digital micropipettor (Ranin, Woburn, MA). The ISO-NOP sensors were connected to an Apollo 4000 Free Radical Analyzer (World Precision Instruments) to make direct electrochemical NO measurements in real time (Davies and Zhang, 2008; Zhang, 2004). Prior to each use, electrodes were calibrated via *S*-nitroso-N-acetyl-D,L-penicillamine (SNAP) decomposition to NO in a copper catalyst solution (cuprous chloride, 0.1M). Data were collected at a rate of 10 samples per second, and measurements were made only during steady-state responses that were at least 30 s in duration. Because the amount of microvascular tissue that was dissected varied between experiments, data were normalized to tissue mass (nM/mg).

Measurement of microvascular oxidative stress. In a separate group of rats, ROS were quantified in the microvascular wall via hydroethidine (HE) oxidation. HE was added to the muscle superfusate at a concentration of 1×10^{-3}M, and the spinotrapezius muscle was continuously exposed to this HE-containing superfusate for 30 min in complete darkness to prevent HE photo-destruction. HE has been extensively used for the detection of O_2^- (Benov *et al*., 1998; Bindokas *et al*., 1996; Morgan *et al*., 1979). HE easily permeates cell membranes and, when oxidized by O_2^-, is converted to fluorescent ethidium bromide that intercalates into nuclear DNA (Benov *et al*., 1998; Morgan *et al*., 1979). In theory, any differences among vessels in the extent of cellular HE loading could also lead to differences in ethidium bromide fluorescence that would be erroneously interpreted as differences in O_2^- activity. To circumvent this problem, we calculated the ratio of oxidized-to-unoxidized substrate in the arteriolar wall from paired fluorescence intensity measurements at the peak emission wavelengths for ethidium bromide and HE, respectively. Tissue autofluorescence at each of these wavelengths was measured before HE exposure, and then subtracted from signals measured after HE exposure to determine specific ethidium bromide and HE fluorescence intensities. After the 30-min exposure period, the muscle was rinsed with normal superfusate for 15 min to remove extracellular HE, and then briefly (1–2 s) illuminated with a mercury lamp, using appropriate excitation and emission filters for detection of ethidium bromide fluorescence (480–550 nm bandpass, 590 nm barrier), and HE fluorescence (330–385 nm bandpass, 420 nm barrier). Fluorescence images were acquired, stored and analyzed with Metamorph 6.01 imaging software (Universal Imaging, Dowington, PA).

Nitrotyrosine staining. In a separate group of rats, the lungs and spinotrapezius muscle were harvested for nitrotyrosine (NT) measurements. This was accomplished with dual-label immunofluorescence for NT and von Willebrand Factor (vWF). The lung was inflated with 2:1 OCT in 20% sucrose/PBS solution and then cut along the mainstem bronchus, embedded in OCT, and frozen in an isopentane slurry on dry ice. The spinotrapezius muscle was embedded in OCT and then frozen in an isopentane slurry on dry ice. Frozen sections of spinotrapezius muscle and lung from rats exposed to 10 μg nano-TiO_2 or air were stained for NT, generally the product of peroxynitrite reactions with cellular proteins. To further demonstrate the localization of NT relative to the vasculature, vascular endothelium was demonstrated by staining for vWF. Sections were cut with a cryostat, fixed in acetone, blocked with 10% donkey serum and incubated overnight in the refrigerator with a primary antibody mixture containing a 1:50 dilution of rabbit anti-NT (Upstate, Temecula, CA) and a 1:200 dilution of sheep anti-vWF (Abcam, Cambridge, MA). The secondaries were Alexa 594-labeled donkey anti-rabbit and Alexa 488-labeled donkey anti-sheep (Invitrogen, Carlsbad, CA). Slides were coverslipped using Prolong mounting media with DAPI (Invitrogen). Using this procedure, NT has red fluorescence, the vascular endothelium has green fluorescence, and nuclei fluoresce blue. The adjacent serial section was stained with Giemsa for identification of inflammatory cells. The negative control sections used rabbit and sheep IgG in place of the primary antibodies and were otherwise treated identically to the sections for dual-label immunofluorescence.

Data and statistical analyses. Arteriolar diameter (D, μm) was sampled at 10-s intervals during all control and infusion periods. Resting vascular tone was calculated for each vessel as follows: Tone (%) = $[(D_{pass} - D_c)/D_{pass}] \times 100$, where D_{pass} is passive diameter under adenosine (ADO) and D_c is the diameter measured during the control period (resting diameter). A tone of 100% represents complete vessel closure, whereas 0% represents the passive state. In order to evaluate arteriolar responsiveness between individual groups with subtle differences in resting diameter, arteriolar diameter was normalized. In this case, arteriolar diameter was expressed as the percent change from control and was calculated for each vessel as follows: Diameter (% change from control) = $[(D_{SS}/D_c) - 1] \times 100$, where D_{SS} is the steady-state diameter achieved during A23187 infusion. All data are reported as means ± SE, where "*n*" represents the number of arterioles evaluated and "*N*" represents the number of rats studied. Statistical analysis was performed by commercially available software (Sigmastat, Systat Software, Inc., San Jose, CA). One-way repeated measures ANOVA was used to determine the effect of a treatment within a group, or differences among groups. Two-way repeated measures ANOVA was used to determine the effects of group, treatment and group-treatment interactions on measured variables. For all ANOVA procedures, the Student-Newman-Keuls method for post hoc analysis was used to isolate pair wise differences among specific groups. Significance was assessed at the 95% confidence level ($p < 0.05$) for all tests.

EXPERIMENTAL PROTOCOLS

Protocol 1

Arteriolar endothelium-dependent dilation was evaluated during intravital microscopy experiments by assessing the capacity for Ca^{2+}-dependent endothelial NO formation in response to intraluminal infusion of the calcium ionophore A23187 as previously described (Nurkiewicz and Boegehold, 2004; Nurkiewicz *et al*., 2006, 2008). Briefly, glass micropipettes were filled with a 10^{-7}M solution of A23187, inserted into the arteriolar lumen, and A23187 was then infused directly into the flow stream for 2-min periods at ejection pressures of 5, 10, 20, and 40 psi. A 2-min recovery period followed each ejection. In some experiments, the following agents were added to the superfusate to inhibit mechanisms that may be affecting NO bioavailability and/or microvascular responsiveness: (1) superoxide and H_2O_2 were scavenged with the superoxide dismutase mimetic 2,2,6,6-tetramethylpiperidine-N-oxyl (TEMPOL, 10^{-4}M final bath

concentration) and catalase (50 U/ml final bath concentration), respectively; (2) MPO was inhibited by tissue superfusion with 4-aminobenzoic hydrazide (ABAH, 10μM final superfusate concentration) for 20 min prior to repeating any experimental procedures; (3) nicotinamide adenine dinucleotide phosphate (NADPH) oxidase was inhibited by tissue superfusion with apocynin (10^{-4}M final superfusate concentration) for 20 min prior to repeating any experimental procedures. At the end of all intravital experiments, ADO was added to the superfusate (10^{-4}M final concentration) to fully dilate the microvascular network and determine the passive diameter of each arteriole studied.

Protocol 2

To evaluate arteriolar responsiveness to NO, the NO donor sodium nitroprusside (SNP) was iontophoretically applied to individual arterioles as previously described (Nurkiewicz *et al.*, 2004). Briefly, glass micropipettes were fabricated as described for Protocol 1, but filled with a 0.05M solution of SNP in distilled water. The pipette tip was placed in light contact with the arteriolar wall, and a current programmer (model 260, World Precision Instruments, Inc.) delivered continuous 2-min ejection currents (5, 10, and 20 nA, randomly). A recovery period of at least 2 min followed each application.

Protocol 3

Endogenous microvascular NO formation was directly measured in suspensions of excised microvessels from each of the exposure groups (and Sham-Controls). NO production was stimulated by introducing a 20 μl of bolus dose of A23187 (10^{-3}M) into the chamber (10^{-5}M final concentration). In these exposure dose-response experiments, NOS activity was then competitively inhibited by coincubation with N^G-monomethyl-L-arginine (L-NMMA, 10^{-4}M final superfusate concentration), and the microvessels were stimulated again with A23187. Time course studies indicated that the microvessels produced reliable NO signals for multiple stimulations, over 2–3 h. Despite this, only two stimulations were performed per experiment, and each experiment lasted less than 1 h.

RESULTS

At the time of experiments, animals were 41–43 days old, and regardless of experimental group, no differences in body weight or blood pressure were observed (Table 1). Similarly, no differences in resting arteriolar diameter, passive diameter or calculated tone were observed among the groups (Table 2). This suggests that regardless of the type of particle inhaled; basal systemic microvascular tone is not perturbed.

Consistent with our previous report (Nurkiewicz *et al.*, 2008), inhalation of TiO_2 nanoparticles significantly impaired endothelium-dependent arteriolar dilation in response to intraluminal infusion of A23187 (Fig. 1). This was most evident at 40 psi where arterioles in the Sham-Control group dilated up to 108 ± 20% of their original diameter. The microvascular responsiveness observed in the Sham-Control group was virtually identical to responses previously noted in naive rats or those intratracheally instilled with saline (Nurkiewicz and Boegehold, 2004; Nurkiewicz *et al.*, 2004). This indicates that housing in the exposure chamber alone does not induce untoward biologic effects. At the particle doses used in the current study (67 μg fine TiO_2, 10 μg nano-TiO_2), equivalent levels of arteriolar dysfunction were found in the two exposure groups. This was most evident at 40 psi where arterioles dilated to only 23 ± 8% and 24 ± 13% of their original diameters in the fine and nano-TiO_2 exposure groups, respectively. These exposure doses were chosen for the current study as they most closely represented the dose (pulmonary deposition for each particle size) at which endothelium-dependent arteriolar dilation was impaired by at least 50% (~EC_{50}) in our previous work (Nurkiewicz *et al.*, 2008). The 40 psi ejection stimulus is highlighted here and used in following experiments because the impact of particle exposure on microvascular function is most evident at this ejection pressure.

After particle exposure, arteriolar dilation in response to abluminal microiontophoretic application of SNP was not different from Sham-Controls (Fig. 2). Arteriolar dilations under these conditions were also not different among exposure groups, and all groups were near their maximal diameters at a current dose of 20 nAmp. These findings are consistent with our previous findings in this microvascular bed after exposure to environmental particles (Nurkiewicz *et al.*, 2004). Collectively, this indicates that vascular smooth muscle sensitivity to NO is not altered after nanoparticle exposure.

Representative bright-field and fluorescent photomicrographs of the spinotrapezius muscle microcirculation are presented in Figures 3A–D. HE treatment of the spinotrapezius

TABLE 1
Profiles of Experimental Animals Used for Intravital Studies

	Exposure parameters					
Dose/group	Aerosol concentration (mg/m^3)	Duration (min)	Number of animals (*N*)	Age (days)	Weight (grams)	Mean arterial pressure (mm Hg)
Sham-Control	0	240	10	43 ± 1	220 ± 14	97 ± 6
67 μg Fine TiO_2	16	300	17	42 ± 1	214 ± 4	98 ± 4
10 μg Nano-TiO_2	6	240	16	41 ± 1	212 ± 4	97 ± 5

TABLE 2
Resting Variables for All Arterioles Studied in Intravital Studies

Dose/group	Number of vessels (*n*)	Resting diameter (μm)	Passive diameter (μm)	Resting tone (% of maximum)
Sham-Control	15	41 ± 2	99 ± 4	58 ± 1
67 μg Fine TiO_2	48	44 ± 2	100 ± 3	56 ± 1
10 μg Nano-TiO_2	45	41 ± 1	93 ± 2	56 ± 1

microcirculation revealed a significant increase in arteriolar ethidium bromide fluorescence (normalized to HE fluorescence) in both particle exposure groups (Fig. 3, bottom). This ratio, as compared with the Sham-Control group (1.03 ± 0.01), was significantly increased after exposure to fine (1.09 ± 0.01) and nano-TiO_2 (1.09 ± 0.01). This increase in fluorescence verifies that the amount of ROS in the microvascular wall is elevated after particle exposure.

Exposure to 10 μg nano-TiO_2 significantly increased the area (μm^2) of tissue containing NT in both the lung (Fig. 4) by threefold and spinotrapezius microcirculation (Fig. 5) by fourfold. In both tissues, indirect immunofluorescence for NT was principally localized within discrete inflammatory cells. Because NT is a product of peroxynitrite-induced tyrosine nitration, the increased NT production that follows particle exposure suggests nitrosative injury within the lung and in the systemic microcirculation.

A bolus dose of A23187 stimulated isolated microvessels from Sham-Control rats to robustly produce NO (33 ± 5 nM/mg, Fig. 6). During coincubation with L-NMMA, this response was significantly inhibited by 65% (to 11 ± 4 nM/mg). This verifies that the majority of the signal produced by the probes under these conditions was NO dependent. Stimulated NO production in isolated microvessels from rats exposed to either fine or nano-TiO_2 was significantly decreased. This impairment was dose-dependent in that as pulmonary particle deposition increased, the ability to produce NO was progressively compromised by 40–85% in the fine TiO_2 groups and 30–88% in the nano-TiO_2 groups. Similar to Sham-Controls, NO production was sensitive to NOS inhibition in that a significant portion of the NO produced under normal conditions was decreased during coincubation with L-NMMA.

In further experiments, a single particle exposure dose was focused upon for each group (fine TiO_2, 67 μg; and nano-TiO_2, 10 μg) to better characterize what oxidant-generating mechanisms may be quenching endogenous NO (Fig. 7). At these exposure doses, stimulated NO production was 8 ± 2 and 10 ± 2 nM/mg for the fine TiO_2 and nano-TiO_2 groups, respectively. Radical scavenging with TEMPOL and catalase similarly and significantly increased stimulated NO production in both groups to 34 ± 5 and 39 ± 12 nM/mg for the fine TiO_2 and nano-TiO_2 groups, respectively. Inhibition of NADPH oxidase with apocynin significantly increased NO production in both groups to 44 ± 11 and 24 ± 7 nM/mg for the fine TiO_2 and nano-TiO_2 groups, respectively. Although the NO response under apocynin was larger in the fine TiO_2 group, the biological relevance of this difference is unclear. Inhibition of MPO with ABAH significantly increased NO production in both groups to 46 ± 12 and 24 ± 6 nM/mg for the fine TiO_2 and nano-TiO_2 groups,

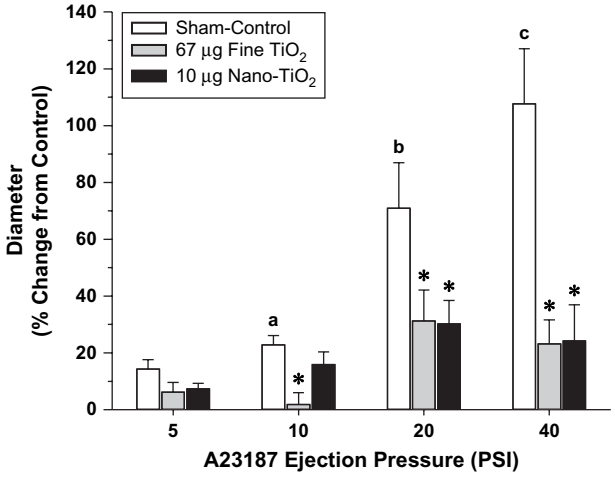

FIG. 1. Intraluminal A23187 infusion produces dose-dependent endothelium-dependent arteriolar dilation that is attenuated by particle inhalation. Sham-control, $n = 8$; 67 μg fine TiO_2, $n = 8$; and 10 μg nano-TiO_2, $n = 10$. (a) $p < 0.05$ versus 5 psi Sham-Control group. (b) $p < 0.05$ versus 10 psi Sham-Control group. (c) $p < 0.05$ versus 20 psi Sham-Control group. *$p < 0.05$ versus Sham-Control group at the same ejection pressure. Values are means ± SE.

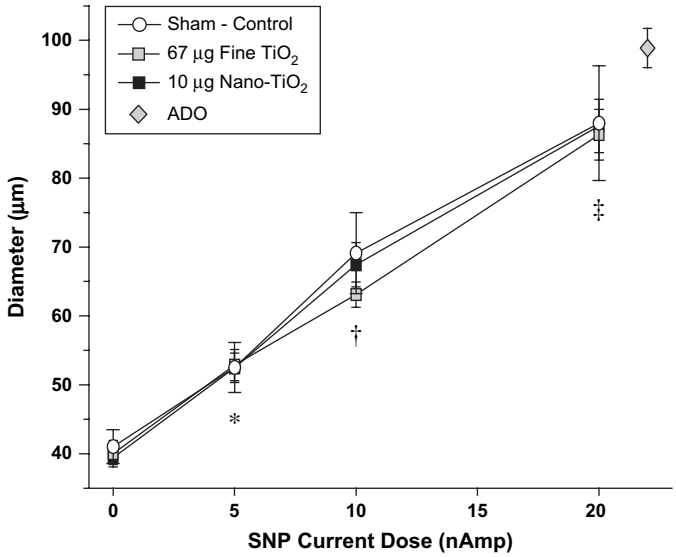

FIG. 2. Arteriolar vascular smooth muscle NO sensitivity is not altered after particle inhalation. SNP was locally applied to individual arterioles via microiontophoresis and produced equivalent dose-dependent dilations in all groups that were near maximal (vs. ADO). Sham-Control, $n = 7$; 67 μg fine TiO_2; $n = 9$, and 10 μg nano-TiO_2, $n = 10$. *$p < 0.05$ versus 0 nAmp for all groups. †$p < 0.05$ versus 5 nAmp for all groups. ‡$p < 0.05$ versus 10 nAmp for all groups. Values are means ± SE.

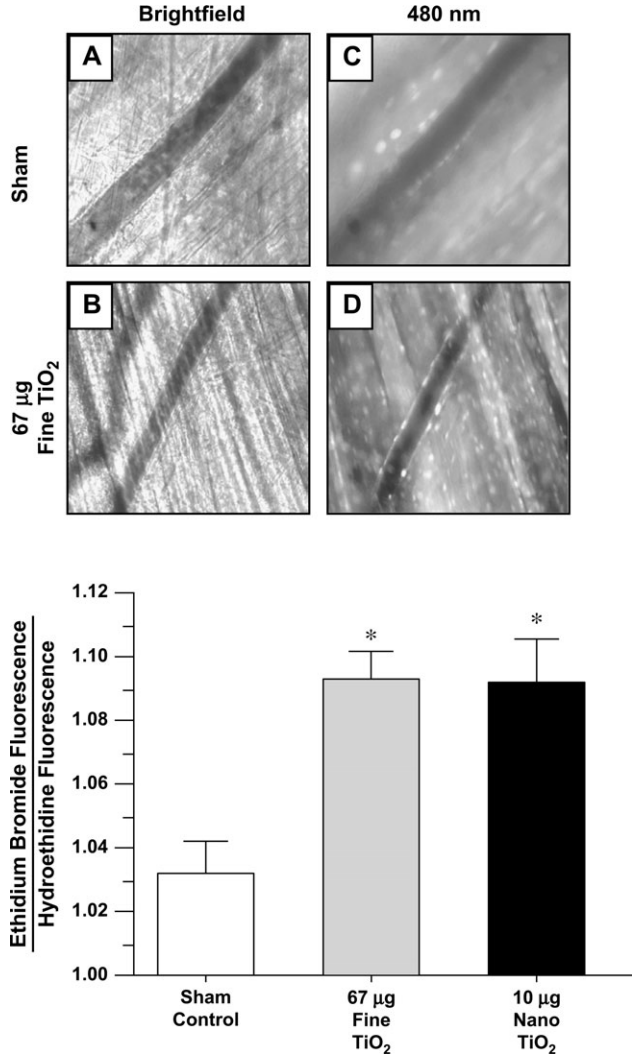

FIG. 3. Particle inhalation increases oxidative stress in the microvascular wall. Top, representative bright-field pictures for the Sham-Control (A) and 67 µg fine TiO_2 groups (B); and illumination at 480 nm for the Sham-Control (C) and 67 µg fine TiO_2 groups (D). Similar images were produced for the 10 µg nano-TiO_2 group (not shown). Bottom, ethidium bromide fluorescence (normalized to background fluorescence, HE). Sham-control, $n = 11$; 67 µg fine TiO_2; $n = 16$, and 10 µg nano-TiO_2, $n = 15$. *$p < 0.05$ versus Sham-Control group. Values are means ± SE.

respectively. Again, although the NO response under ABAH was more potent in the fine TiO_2 group, the biological relevance of this difference is unclear. These agents did not significantly alter NO production in the Sham-Control group (data not shown).

In Figure 8, the agents used to enhance stimulated NO production were superfused over the spinotrapezius muscle in order to evaluate their effectiveness on restoring endothelium-dependent arteriolar dilation. Under control conditions with the normal superfusate, A23187 infusion (40 psi) produced significant arteriolar dilation in the Sham-Control group (108 ± 19% increase from control diameter). After exposure to either fine or nano-TiO_2, arteriolar dilation was limited to only 10 ± 5% or 20 ± 4% above control diameter, respectively. Radical scavenging with TEMPOL and catalase partially restored arteriolar dilation in both groups (increases from the control diameter of 58 ± 5% and 79 ± 11% for the fine TiO_2, and nano-TiO_2 groups, respectively). NADPH oxidase inhibition with apocynin also partially restored arteriolar dilation in both groups (increases from the control diameter of 85 ± 9% and 85 ± 10% for the fine TiO_2, and nano-TiO_2 groups, respectively). MPO inhibition with ABAH was also capable of partially restoring arteriolar dilation in both groups (increases from the control diameter of 46 ± 5% and 76 ± 6% for the fine TiO_2, and nano-TiO_2 groups, respectively). These agents did not significantly alter arteriolar dilation in the Sham-Control group (data not shown).

DISCUSSION

The critical findings in the current study are threefold: first, microvascular NO bioavailability is compromised after nanoparticle exposure; second, nanoparticle exposure increases ROS and RNS production in the microvascular wall; and third, the microvascular dysfunction and decrease in NO bioavailability that follow nanoparticle exposure are directly linked with discrete radical-generating mechanisms. These findings are particularly relevant to humans in that numerous studies have implicated the role of NO, as well as oxidative stress in PM-dependent vascular dysfunction, but for obvious reasons, are unable to make such direct measurements (Briet *et al.*, 2007; Brook *et al.*, 2002; Mills *et al.*, 2005; Schneider *et al.*, 2008; Tornqvist *et al.*, 2007).

We have recently reported that compared with fine PM, at a similar mass pulmonary deposition, nanoparticle inhalation produces significantly greater microvascular dysfunction (Nurkiewicz *et al.*, 2008). This conclusion was reached by comparing microvascular reactivity between multiple groups of rats exposed to five doses of nano-TiO_2 (4–38 µg depositions) or five doses of fine TiO_2 (8–90 µg depositions). Collectively, these pulmonary doses/depositions and microvascular responses were used to establish the EC_{50} of 67 µg fine TiO_2 and 10 µg nano-TiO_2 doses used in the current study (i.e., these doses impaired microvascular reactivity by ~50% in each group). The issue of nanotoxicity is most evident among our data in that it required a fine particle deposition that was more than six times greater than the nanoparticle deposition to produce equivalent levels of microvascular dysfunction (67 µg fine TiO_2 vs. 10 µg nano-TiO_2, Fig. 1), oxidative stress (Fig. 3) and NO quenching (Fig. 6). Whether or not pulmonary mass deposition is the most appropriate metric to use for comparing such distinctly different particles remains to be determined (Warheit *et al.*, 2007). In the absence of a definitive answer to this issue, and in order to establish relevance to human exposures; it is important to define the aerosol concentrations

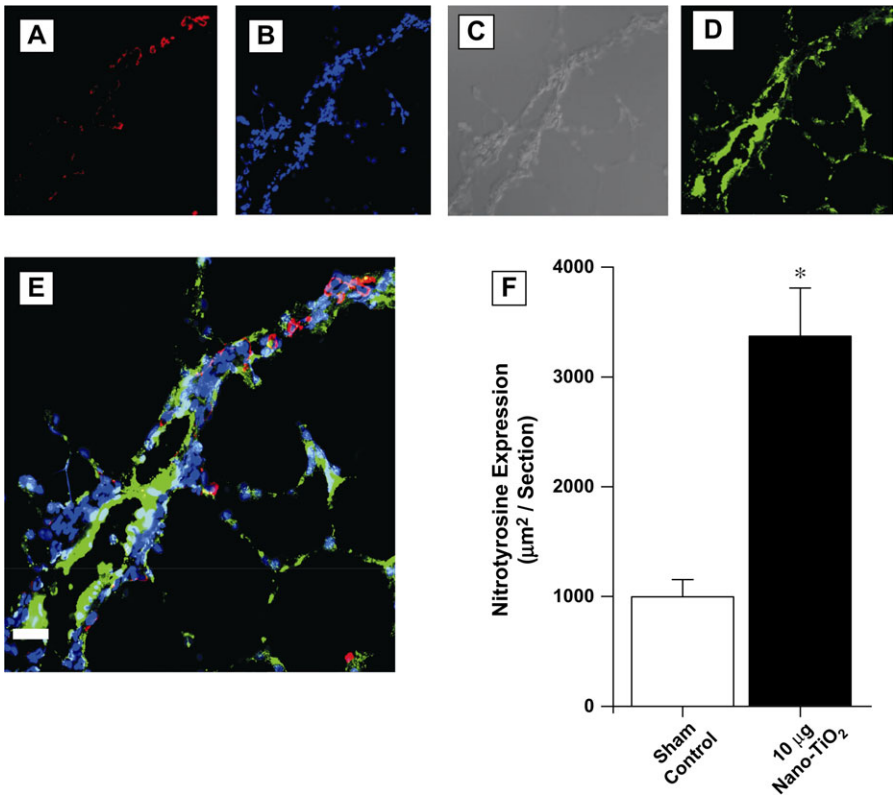

FIG. 4. Indirect immunofluorescent and DIC confocal microscopy images (representative) of the lung and intrapulmonary vasculature from a rat exposed to 10 μg nano-TiO_2. (A) Red fluorescence demonstrates NT and is localized within individual cells morphologically consistent with inflammatory cells. (B) Blue fluorescence is DAPI labeling of nuclei. (C) Differential Interference Contrast (DIC) confocal microscopy demonstrating lung structure with a large vessel traversing the section. (D) Green fluorescence cells indicates vWF, a marker of vascular endothelium. (E) Triple label immunofluorescence. Coexpression of green and red gives a yellow color and indicates that these markers are within the same location. The majority of pulmonary NT expression is within discrete inflammatory cells in alveoli or near but only occasionally within the vascular endothelium (bar is 20 micrometers). (F) NT expression in the lung was increased by TiO_2 inhalation. Data are from Sham-Control, $n = 4$; and 10 μg nano-TiO_2, $n = 6$; three fields per slide. Values are means ± SE. *$p < 0.05$ versus sham/control.

and exposure times used in the current study to produce our groups in a single exposure (5 h at 16 mg/m^3 and 4 h at 6 mg/m^3 for fine TiO_2 and nano-TiO_2, respectively). The current occupational exposure limit to fine TiO_2 is 5 mg/m^3. Therefore, a worker exposed at this level would achieve a pulmonary burden equivalent to 67 μg in the rat (normalized for alveolar epithelial surface area, Stone *et al.*, 1992, and taking human pulmonary deposition of a 1 μm particle of 20%, Bates *et al.*, 1966) within 5 working days. Levels of nano-TiO_2 have been measured in a production plant to be as high as 1.4 μg/m^3 (NIOSH, personal communication). Therefore, workers exposed at this level could achieve a pulmonary burden equivalent to 10 μg in the rat (normalized for alveolar epithelial surface area and assuming a deposition fraction of 45%) within 5 years.

Without appropriate particle characterization, it is difficult to compare findings between toxicological studies or generalize implications in regards to environmental or occupational health (Warheit, 2008). Indeed, we have characterized the particles used in the current study, as well as documented the aerosol profiles of all doses used (see Methods, "Inhalation Exposure" as well as Nurkiewicz *et al.*, 2008). The particles used herein are of different phase compositions; fine TiO_2 was ~99% rutile, whereas nano-TiO_2 was an 80/20 mixture of anatase and rutile, respectively. The anatase phase of TiO_2 has been suggested to be more cytotoxic than the rutile phase (Sayes *et al.*, 2006). Because we used differently sized particles, of different phase compositions, it may seem difficult, if not impossible to distinguish the effects of particle size on microvascular function. However, it is important to note that increased cytotoxicity of the anatase phase of TiO_2 (compared with rutile) is directly related to UV illumination of the particles; and this effect is largely a function of UV light wavelength (Cai *et al.*, 1991) as well as duration (Zhang and Sun, 2004). It is perhaps more important to note that the biologic effects of UV stimulated TiO_2 particles are highly dependent on the concentration of active particles (Nakagawa *et al.*, 1997; Sayes *et al.*, 2006). We did not UV stimulate any of the TiO_2 particles used in the current study, and because our inhalation facility as well as particle storage location are devoid of windows, the likelihood for accidental UV illumination is very low, if not non-existent. Moreover, the particle doses used herein (even if we consider 100% particle migration to the systemic

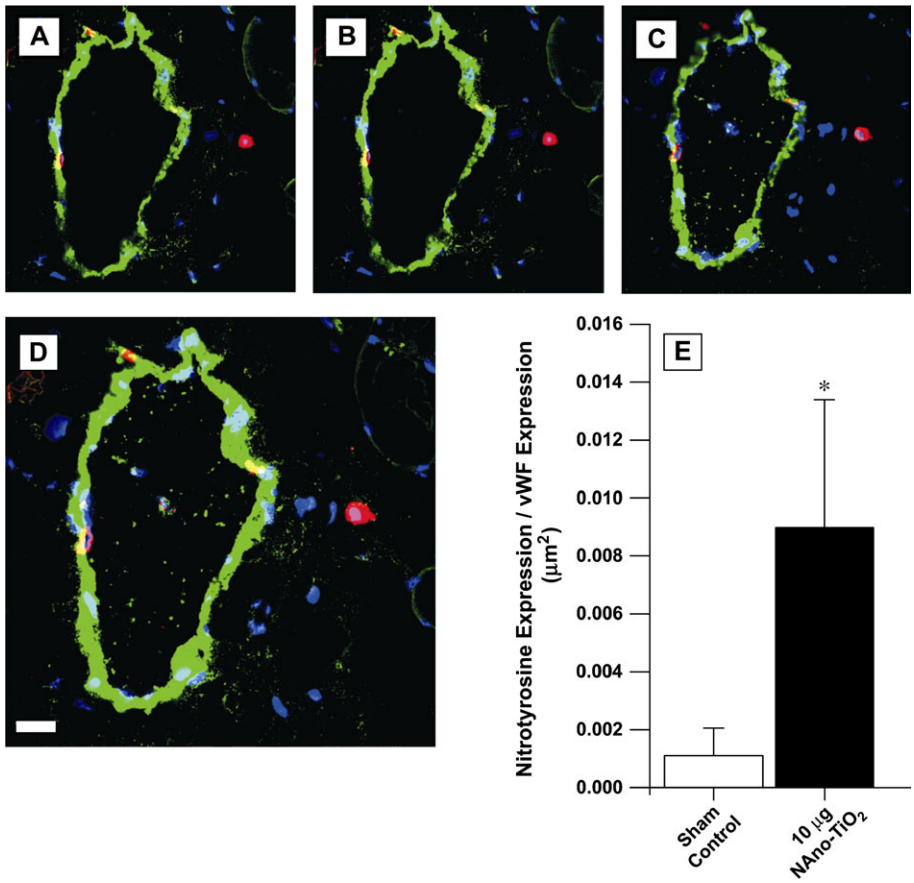

FIG. 5. Indirect immunofluorescent confocal microscopy images (representative) of the spinotrapezius muscle from a rat exposed to 10 μg nano-TiO_2. Red fluorescence demonstrates NT and is localized within individual cells morphologically consistent with inflammatory cells. Green fluorescence cells indicates von Willebrand Factor, a marker of vascular endothelium. Coexpression of green and red gives a yellow color and indicates that these markers are within the same location. (A–C) From a Z-stack, indicating that NT is running longitudinally through the microvascular wall. Panel D is the top of the stack (bar is 20 μm). (E) NT expression in the spinotrapezius muscle microcirculation was increased after nano-TiO_2 inhalation. Data are from Sham-Control, $n = 4$; and 10 μg nano-TiO_2, $n = 6$; one field per slide. Values are means ± SE. *$p < 0.05$ versus Sham/Control.

circulation) are well below the "no effect" doses noted by both Nakagawa *et al.* (1997) and Sayes *et al.* (2006). Therefore, it appears more likely that the microvascular dysfunction that follows particle exposure is a function of particle size, rather than particle phase.

The microvascular dysfunction associated with exposure to either fine TiO_2 or nano-TiO_2 is not due to altered arteriolar smooth muscle responsiveness to NO (Fig. 2). We have previously shown this to also be the case after exposure to residual oil fly ash (Nurkiewicz *et al.*, 2004). Our finding of an unaltered smooth muscle NO sensitivity after particle exposure is in agreement with findings in the rabbit carotid artery (Tamagawa *et al.*, 2008), and mouse mesenteric artery and vein (Knuckles *et al.*, 2008), but not the mouse coronary septal artery (Campen *et al.*, 2005), rat aorta (Bagate *et al.*, 2004), or intrapulmonary artery (Courtois *et al.*, 2008). Multiple possibilities exist for this disparity in smooth muscle sensitivity after particle exposure. First, the various tissues used possess inherently different levels of function as well as vascular reactivity that under certain artificial conditions prevent meaningful comparisons. However, studies do exist that report divergent sensitivities to different NO donors in the same vascular segment (Courtois *et al.*, 2008). Second, the NO donors used across experiments can be different. In the current study, we used SNP which donates NO via interaction with a biological membrane at physiological pH (Butler and Megson, 2002; Ignarro *et al.*, 2002). Whereas, diazeniumdiolates such as diethylamino-NONOate spontaneously release NO in a more controlled fashion (Ignarro *et al.*, 2002; Miranda *et al.*, 2005). Despite different mechanisms of NO donation, studies in the basilar and carotid arteries indicate that SNP is as effective, if not one of the most potent NO donators (Salom *et al.*, 1998, 1999). Ultimately, it is the activity of cyclic guanosine monophosphate (cGMP) in the VSM that is important in this regard; and studies with cGMP analogs indicate that particle exposure does not alter this sensitivity (Courtois *et al.*, 2008). Third, the particles and conditions used in these and other studies are very different. The potential for

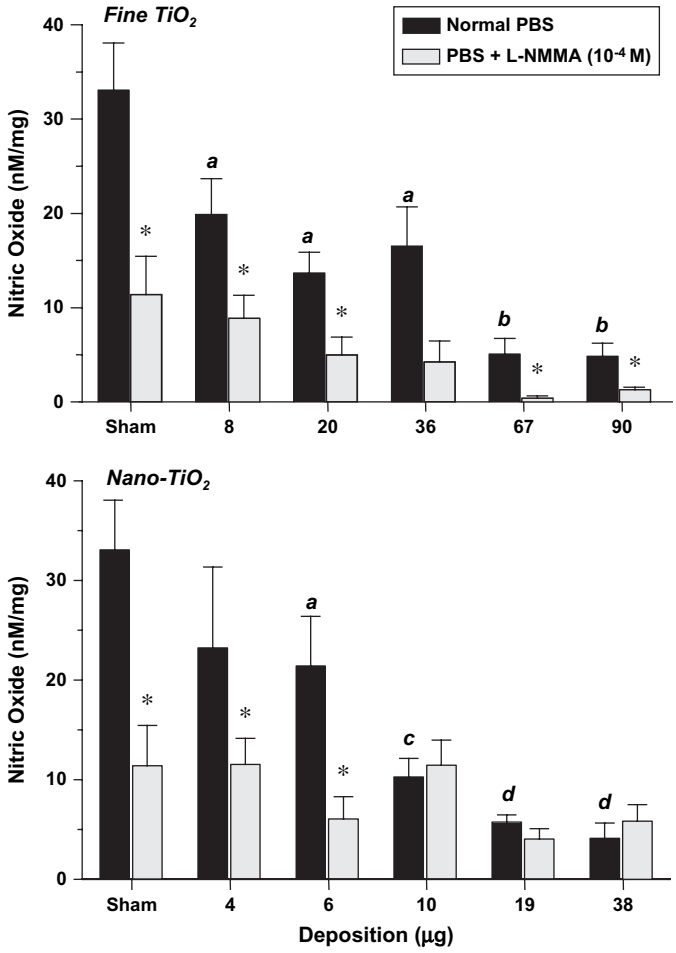

FIG. 6. Endogenous microvascular NO production is attenuated after particle inhalation in a dose-dependent manner. Endothelial NO production was stimulated by a bolus dose of A23187 and measured real time with an electrochemical sensor. NOS inhibition was accomplished by coincubation with L-NMMA during measurements. Top panel, fine TiO_2: 8 μg, $n = 9$; 20 μg, $n = 9$; 36 μg, $n = 7$; 67 μg, $n = 8$; 90 μg, $n = 9$; Sham-Control, $n = 34$. Bottom panel, nano-TiO_2: 4 μg, $n = 6$; 6 μg, $n = 8$; 10 μg, $n = 6$; 19 μg, $n = 6$; 38 μg, $n = 6$; Sham-Control, $n = 34$. a, $p < 0.05$ versus Sham-Control group. b, $p < 0.05$ versus 36 μg fine TiO_2 group. c, $p < 0.05$ versus 6 μg nano-TiO_2 group. d, $p < 0.05$ versus 10 μg nano-TiO_2 group. *$p < 0.05$ versus normal PBS in the same group. Values are means ± SE.

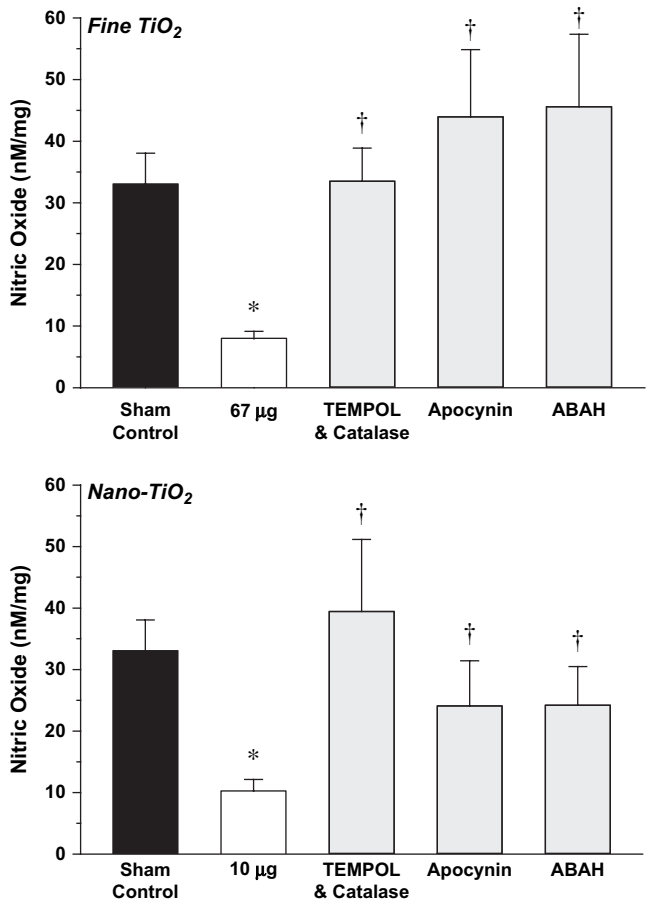

FIG. 7. Radical scavenging or enzyme inhibition restores endogenous NO production after particle exposure. Endothelial NO production was stimulated by a bolus dose of A23187 and measured real time with an electrochemical sensor. Radical scavenging, NADPH oxidase and myeloperoxidase inhibition were accomplished by coincubation with TEMPOL/catalase, apocynin or ABAH, respectively, during measurements. Top panel: Sham-Control, $n = 34$; 67 μg fine TiO_2, $n = 32$; TEMPOL/catalase, $n = 18$; apocynin, $n = 10$; ABAH, $n = 15$. Bottom panel: Sham-Control, $n = 34$; 10 μg nano-TiO_2, $n = 38$; TEMPOL/catalase, $n = 12$; apocynin, $n = 12$; ABAH, $n = 14$. *$p < 0.05$ versus Sham-Control group. †$p < 0.05$ versus 67 μg fine TiO_2 or 10 μg nano-TiO_2 in the same panel. Values are means ± SE.

one technique, particle or emission condition to affect smooth muscle NO sensitivity, while another does not, is high because numerous biological mechanisms have been identified and/or advanced to help explain how a particle of pulmonary origin can influence a systemic tissue (Brook *et al*., 2004; Donaldson *et al*., 2005; Dreher *et al*., 1997; Godleski *et al*., 2000; Oberdorster *et al*., 2004; Watkinson *et al*., 2001).

Microvascular oxidative stress is significantly increased after particle exposure (Fig. 3). This finding is consistent with recent findings in the aortic wall (Sun *et al*., 2008). An elevation of local ROS may potentially consume endothelium derived NO and result in peroxynitrite radical formation (Forstermann and Munzel, 2006). A stable endpoint of peroxynitrite reactions is the formation of NT (Beckman, 1996; Beckman and Koppenol, 1996). In Figure 5, microvascular NT formation is significantly increased in the microvascular wall after particle exposure. Taken together, these findings suggest that following particle exposure, oxidative and nitrosative stress in the microvascular wall consumes endothelial NO.

The logical corollary of the above findings is that endogenous NO production will be compromised after particle exposure (due to radical quenching). Indeed, endogenous microvascular NO production is compromised after particle exposure in a dose-dependent relationship (Fig. 6). To our knowledge, this is the first study to directly measure endogenous NO in real time and report that particle exposure attenuates this measurement. Because our first report that microvascular endothelium-dependent dilation is compromised

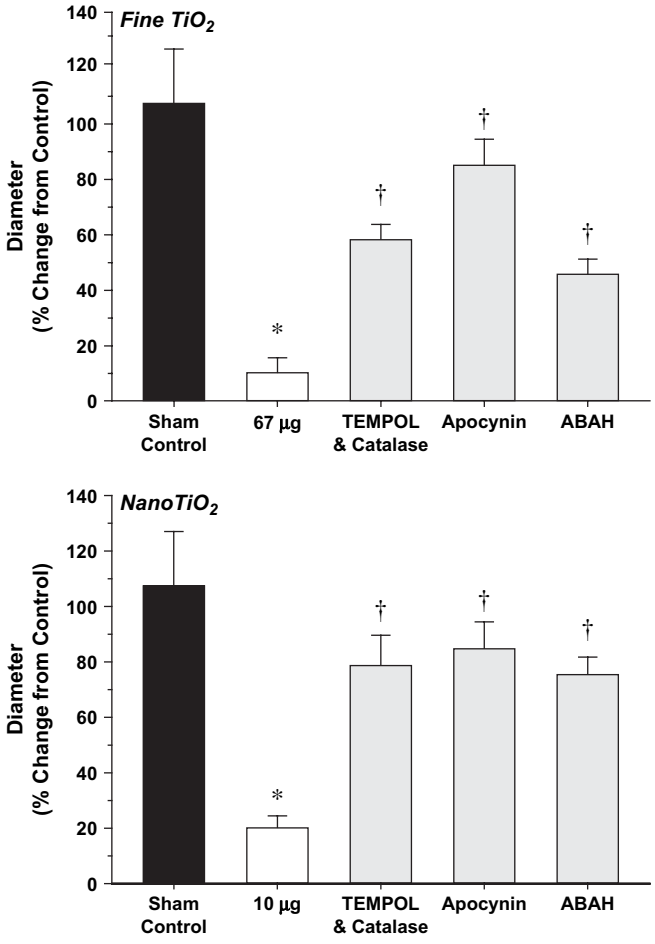

FIG. 8. Radical scavenging or enzyme inhibition restores arteriolar endothelium-dependent dilation after particle exposure. Responses were stimulated by intraluminal infusion of A23187 at 40 psi. Radical scavenging, NADPH oxidase, and myeloperoxidase inhibition were accomplished by coincubation with TEMPOL/catalase, apocynin or ABAH respectively, during measurements. Top panel: Sham-Control, $n = 8$; 67 µg fine TiO_2, $n = 8$; TEMPOL/catalase, $n = 8$; apocynin, $n = 9$; ABAH, $n = 7$. Bottom panel: Sham-Control, $n = 8$; 10 µg nano-TiO_2, $n = 10$; TEMPOL/catalase, $n = 10$; apocynin, $n = 12$; ABAH, $n = 11$, $*p < 0.05$ versus Sham-Control group. $\dagger p < 0.05$ versus 67 µg fine TiO_2 or 10 µg nano-TiO_2 in the same panel. Values are means ± SE.

after particle exposure (Nurkiewicz *et al.*, 2004), it has become obvious that this effect is not limited to the microcirculation (Campen *et al.*, 2005; Hansen *et al.*, 2007; Knuckles *et al.*, 2008; Mills *et al.*, 2005; Rundell *et al.*, 2007). Although the vascular effect is clearly not targeting a singular level of the vasculature, it is imperative to indicate that endothelial stimulation produces numerous vasoactive agents other than NO, including cycloxygenase products, bradykinin, endothelium-derived hyperpolarizing factor, angiotensin, and endothelin. Moreover, the relative contribution of NO versus that of other vasodilators to endothelium-dependent dilation can be very different between vascular beds and even species. Therefore, it is not only critical to directly measure NO in the current studies, but also characterize how the influence of other vasoactive agents is altered after particle exposure.

Making direct NO measurements are time consuming and particularly demanding experiments that, as with all experimental techniques, carry limitations (Davies and Zhang, 2008; Zhang, 2004). Additionally, NO sensors can be unreliable and sensitive to numerous artifacts. We have taken extreme caution in designing our experiments to avoid such complications. Specifically, the NO sensors used in the current study were calibrated before each experiment and no less than two sensors were simultaneously used in a single experiment (to verify that readings were not erroneous). The probes were also randomly calibrated throughout their lifespan (typically less than 2 weeks). Any probe that failed to consistently generate current (in the presence of SNAP) comparable to the standard produced by fresh probes was removed. Perhaps a more important assumption we have made is that the NO measurements should be considered in a nominal sense, rather than attempting to precisely quantify the relationship between pulmonary deposition and microvascular NO production. In this regard, we caution the reader to interpret our findings only in the regard that the exposure doses used herein produce a significant decrease in endogenous microvascular NO production. The presence of artifact may be apparent in Figure 6 where the probes still measured an NO signal in the presence of L-NMMA. However, because this residual NO signal (in the presence of L-NMMA) was variable across the particle types and doses, it can be argued that NOS inhibition was incomplete under these conditions (L-NMMA is not infinitely permeable). Because we have shown that the L-NMMA concentration (10^{-4}M) and incubation time (20 min) used in the current studies maximally inhibits spinotrapezius muscle arteriolar responsiveness to acetylcholine (Boegehold, 1995), incomplete NOS inhibition is unlikely. Given that the NO probes operate in the picoampere range, and the biosensing chamber contained a stir bar that was required to be active for our measurements; it appears more likely that background electrical noise contributed to the residual NO signal that persisted during NOS inhibition.

Given that particle exposure compromises endogenous NO production (Fig. 6), it is essential to determine the fate of NO under this condition. In Figure 3, an increase in microvascular ROS is apparent after particle exposure. Because ROS are capable of consuming NO (Forstermann and Munzel, 2006), we chose to indiscriminately scavenge radicals with TEMPOL and facilitate their ultimate conversion to H_2O via catalase. TEMPOL and catalase incubation partially restored endogenous NO production after exposure to either fine TiO_2 or nano-TiO_2 (Fig. 7). Because HE has been used a probe for superoxide (Benov *et al.*, 1998), it is reasonable to expect that a significant portion of the local ROS that was scavenged by TEMPOL was superoxide. The next logical step in this process was to determine the source of elevated superoxide. Superoxide generation can originate from NADPH oxidase activity

(Sumimoto, 2008), and apocynin has been shown to inhibit this activity (Johnson *et al*., 2002). In our experiments, apocynin incubation partially restored endogenous NO production after exposure to either fine TiO_2 or nano-TiO_2 (Fig. 7). Myeloperoxidase is also capable of reducing bioavailable NO via generation of reactive substrate radicals (Eiserich *et al*., 2002), or chlorination of L-arginine (Zhang *et al*., 2001). Incubation with the MPO inhibitor ABAH also partially restored endogenous NO production after exposure to either fine TiO_2 or nano-TiO_2 (Fig. 7). Simultaneous incubation with ABAH, TEMPOL and catalase did not produce a greater restoration of NO production (data not shown). This observation suggests that the majority of MPO dependent microvascular dysfunction that follows particle exposure is due to radical generation, rather than decreasing the NOS substrate (L-arginine). The ultimate test of physiological relevance in this regard is whether these ROS scavengers/inhibitors are capable of restoring normal microvascular function after particle exposure. Indeed, incubation of the spinotrapezius muscle with each agent (TEMPOL/catalase, apocynin, ABAH) partially restores arteriolar endothelium-dilation in rats exposed to either fine TiO_2 or nano-TiO_2 (Fig. 8). It is important to note for both NO production and microvascular function that our description of partial restoration (of either response) should be interpreted as the given treatment failed to completely restore either NO production or microvascular function. In this regard, the remaining dysfunction under those conditions may be due to some mechanism that has yet to be identified.

CONCLUSIONS

In the absence of the appropriate particle dose-metric, the current study compared the biologic effects of pulmonary exposure to fine particles and nanoparticles based upon their documented ability to cause microvascular dysfunction in a dose-dependent manner. This dose was essentially an EC_{50}, and the fact that the fine particle dose was more than six times greater than the nanoparticle dose in all experiments, highlights the inherent toxic potential of nanoparticles. Because endogenous NO production, its mechanisms of susceptibility, and the partial restoration of microvascular function after exposure are similar after pulmonary exposure to either fine particles or nanoparticles; it appears that these two particles exert their biologic effects through similar mechanisms. However, it should be considered that even the discrete mechanisms reported herein arise from very complex backgrounds and further studies must venture to this level of mechanistic detail. In regards to normal physiology, blocking these mechanisms only partially restored normal microvascular function in particle exposed animals. Future investigations must bear in mind that it is unlikely that the remaining mechanisms contributing to these effects are related to oxidative or nitrosative stress, NO or even inflammatory mechanisms.

FUNDING

National Institutes of Health/National Institute for Environmental Health Sciences (grant number R01-ES015022) to T.R.N.; and the Health Effects Institute (grant number #4730) to T.R.N.

ACKNOWLEDGMENTS

We thank Lori Battelli, Jared Cumpston, Michelle Donlin, Sherri Friend, Caroll McBride, Amy Moseley, and Kimberly Wix for their expert technical assistance in this study. We also thank Travis Knuckles, Ph.D. and Amanda LeBlanc, Ph.D. for their critical review of this manuscript.

Disclaimers: The findings and conclusions in this report are those of the authors and do not necessarily represent the views of the National Institute for Occupational Safety and Health.

Research described in this article was conducted under contract to the Health Effects Institute (HEI), and organization jointly funded by the United States Environmental Protection Agency (EPA) (Assistance Award No. R-82811201) and certain motor vehicle and engine manufacturers. The contents of this article do not necessarily reflect the views of HEI, or its sponsors, nor do they necessarily reflect the views and policies of the EPA or motor vehicle and engine manufacturers.

REFERENCES

Bagate, K., Meiring, J. J., Gerlofs-Nijland, M. E., Vincent, R., Cassee, F. R., and Borm, P. J. (2004). Vascular effects of ambient particulate matter instillation in spontaneous hypertensive rats. *Toxicol. Appl. Pharmacol*. **197,** 29–39.

Bates, D. V., Fish, B. R., Hatch, T. F., Mercer, T. T., and Morrow, P. E. (1966). Deposition and retention models for internal dosimetry of the human respiratory tract. Task group on lung dynamics. *Health Phys*. **12,** 173–207.

Beckman, J. S. (1996). Oxidative damage and tyrosine nitration from peroxynitrite. *Chem. Res. Toxicol*. **9,** 836–844.

Beckman, J. S., and Koppenol, W. H. (1996). Nitric oxide, superoxide, and peroxynitrite: The good, the bad, and ugly. *Am. J. Physiol*. **271**(5 Pt 1), C1424–C1437.

Benov, L., Sztejnberg, L., and Fridovich, I. (1998). Critical evaluation of the use of hydroethidine as a measure of superoxide anion radical. *Free Radic. Biol. Med*. **25,** 826–831.

Bindokas, V. P., Jordan, J., Lee, C. C., and Miller, R. J. (1996). Superoxide production in rat hippocampal neurons: Selective imaging with hydroethidine. *J. Neurosci*. **16,** 1324–1336.

Boegehold, M. A. (1995). Flow-dependent arteriolar dilation in normotensive rats fed low- or high-salt diets. *Am. J. Physiol*. **269,** H1407–14.

Boegehold, M. A., and Bohlen, H. G. (1988). Arteriolar diameter and tissue oxygen tension during muscle contraction in hypertensive rats. *Hypertension* **12,** 184–91.

Bohlen, H. G., and Lash, J. M. (1996). Intestinal absorption of sodium and nitric oxide-dependent vasodilation interact to dominate resting vascular resistance. *Circ. Res*. **78,** 231–237.

Briet, M., Collin, C., Laurent, S., Tan, A., Azizi, M., Agharazii, M., Jeunemaitre, X., henc-Gelas, F., and Boutouyrie, P. (2007). Endothelial

function and chronic exposure to air pollution in normal male subjects. *Hypertension* **50,** 970–976.

Brook, R. D., Brook, J. R., Urch, B., Vincent, R., Rajagopalan, S., and Silverman, F. (2002). Inhalation of fine particulate air pollution and ozone causes acute arterial vasoconstriction in healthy adults. *Circulation* **105,** 1534–1536.

Brook, R. D., Franklin, B., Cascio, W., Hong, Y., Howard, G., Lipsett, M., Luepker, R., Mittleman, M., Samet, J., Smith, S. C., Jr, *et al*. (2004). Air pollution and cardiovascular disease: A statement for healthcare professionals from the Expert Panel on Population and Prevention Science of the American Heart Association. *Circulation* **109,** 2655–2671.

Brunauer, S., Emmett, P. H., and Teller, E. (1938). Adsorption of gases in multimolecular layers. *J. Am. Chem. Soc.* **60,** 309–319.

Butler, A. R., and Megson, I. L. (2002). Non-heme iron nitrosyls in biology. *Chem. Rev.* **102,** 1155–1166.

Cai, R., Hashimoto, K., Itoh, K., Kubota, Y., and Fujishima, A. (1991). Photokilling of malignant cells with ultrafine TiO2 powder. *Bull. Chem. Soc. Jpn.* **64,** 1268–1273.

Campen, M. J., Babu, N. S., Helms, G. A., Pett, S., Wernly, J., Mehran, R., and McDonald, J. D. (2005). Nonparticulate components of diesel exhaust promote constriction in coronary arteries from ApoE−/− Mice. *Toxicol. Sci.* **88,** 95–102.

Courtois, A., Andujar, P., Ladeiro, Y., Baudrimont, I., Delannoy, E., Leblais, V., Begueret, H., Galland, M. A., Brochard, P., Marano, F., *et al*. (2008). Impairment of NO-dependent relaxation in intralobar pulmonary arteries: Comparison of urban particulate matter and manufactured nanoparticles. *Environ. Health Perspect.* **116,** 1294–1299.

Cozzi, E., Hazarika, S., Stallings, H. W., III, Cascio, W. E., Devlin, R. B., Lust, R. M., Wingard, C. J., and Van Scott, M. R. (2006). Ultrafine particulate matter exposure augments ischemia-reperfusion injury in mice. *Am. J. Physiol. Heart Circ. Physiol.* **291,** H894–H903.

Davies, I. R., and Zhang, X. (2008). Nitric oxide selective electrodes. *Methods Enzymol.* **436,** 63–95.

Dockery, D. W., Pope, C. A., III, Xu, X., Spengler, J. D., Ware, J. H., Fay, M. E., Ferris, B. G., Jr, and Speizer, F. E. (1993). An association between air pollution and mortality in six U.S. cities. *N. Engl. J. Med.* **329,** 1753–1759.

Donaldson, K., Tran, L., Jimenez, L. A., Duffin, R., Newby, D. E., Mills, N., MacNee, W., and Stone, V. (2005). Combustion-derived nanoparticles: A review of their toxicology following inhalation exposure. *Part Fibre. Toxicol.* **2,** 10.

Dreher, K. L., Jaskot, R. H., Lehmann, J. R., Richards, J. H., McGee, J. K., Ghio, A. J., and Costa, D. L. (1997). Soluble transition metals mediate residual oil fly ash induced acute lung injury. *J. Toxicol. Environ. Health* **50,** 285–305.

Eiserich, J. P., Baldus, S., Brennan, M. L., Ma, W., Zhang, C., Tousson, A., Castro, L., Lusis, A. J., Nauseef, W. M., White, C. R., *et al*. (2002). Myeloperoxidase, a leukocyte-derived vascular NO oxidase. *Science* **296,** 2391–2394.

Forstermann, U., and Munzel, T. (2006). Endothelial nitric oxide synthase in vascular disease: From marvel to menace. *Circulation* **113,** 1708–1714.

Godleski, J. J., Verrier, R. L., Koutrakis, P., Catalano, P., Coull, B., Reinisch, U., Lovett, E. G., Lawrence, J., Murthy, G. G., Wolfson, J. M., *et al*. (2000). Mechanisms of morbidity and mortality from exposure to ambient air particles. *Res. Rep. Health Eff. Inst.* **91,** 5–88.

Hansen, C. S., Sheykhzade, M., Moller, P., Folkmann, J. K., Amtorp, O., Jonassen, T., and Loft, S. (2007). Diesel exhaust particles induce endothelial dysfunction in apoE−/− mice. *Toxicol. Appl. Pharmacol.* **219,** 24–32.

Hurum, D. C., Agrios, A. G., Gray, K. A., Rajh, T., and Thurnauer, M. C. (2003). Recombination pathways in the Degussa P25 formulation of TiO2: Surface versus lattice mechanisms. *J. Phys. Chem. B* **107,** 4545–4549.

Ignarro, L. J., Napoli, C., and Loscalzo, J. (2002). Nitric oxide donors and cardiovascular agents modulating the bioactivity of nitric oxide: An overview. *Circ. Res.* **90,** 21–28.

Johnson, D. K., Schillinger, K. J., Kwait, D. M., Hughes, C. V., McNamara, E. J., Ishmael, F., O'Donnell, R. W., Chang, M. M., Hogg, M. G., Dordick, J. S., Santhanam, L., Ziegler, L. M., *et al*. (2002). Inhibition of NADPH oxidase activation in endothelial cells by ortho-methoxy-substituted catechols. *Endothelium* **9,** 191–203.

Knuckles, T. L., Lund, A. K., Lucas, S. N., and Campen, M. J. (2008). Diesel exhaust exposure enhances venoconstriction via uncoupling of eNOS. *Toxicol. Appl. Pharmacol.* **230,** 346–351.

Matsunaga, T., Weihrauch, D. W., Moniz, M. C., Tessmer, J., Warltier, D. C., and Chilian, W. M. (2002). Angiostatin inhibits coronary angiogenesis during impaired production of nitric oxide. *Circulation* **105,** 2185–2191.

Mills, N. L., Tornqvist, H., Robinson, S. D., Gonzalez, M., Darnley, K., MacNee, W., Boon, N. A., Donaldson, K., Blomberg, A., Sandstrom, T., and Newby, D. E. (2005). Diesel exhaust inhalation causes vascular dysfunction and impaired endogenous fibrinolysis. *Circulation* **112,** 3930–3936.

Miranda, K. M., Katori, T., Torres de Holding, C. L., Thomas, L., Ridnour, L. A., McLendon, W. J., Cologna, S. M., Dutton, A. S., Champion, H. C., Mancardi, D., *et al*. (2005). Comparison of the NO and HNO donating properties of diazeniumdiolates: Primary amine adducts release HNO in Vivo. *J. Med. Chem.* **48,** 8220–8228.

Morgan, A. R., Evans, D. H., Lee, J. S., and Pulleyblank, D. E. (1979). Review: Ethidium fluorescence assay. Part II. Enzymatic studies and DNA-protein interactions. *Nucleic Acids Res.* **7,** 571–594.

Nabah, Y. N., Mateo, T., Cerdyicoly, M., Alvarez, A., Martinez, M., Issekutz, A. C., and Sanz, M. J. (2005). L-NAME induces direct arteriolar leukocyte adhesion, which is mainly mediated by angiotensin-II. *Microcirculation.* **12,** 443–453.

Nakagawa, Y., Wakuri, S., Sakamoto, K., and Tanaka, N. (1997). The photogenotoxicity of titanium dioxide particles. *Mutat. Res.* **394,** 125–132.

Nurkiewicz, T. R., and Boegehold, M. A. (2004). Calcium-independent release of endothelial nitric oxide: Onset during rapid juvenile growth. *Microcirculation.* **11,** 453–462.

Nurkiewicz, T. R., Porter, D. W., Barger, M., Castranova, V., and Boegehold, M. A. (2004). Particulate matter exposure impairs systemic microvascular endothelium-dependent dilation. *Environ. Health Perspect.* **112,** 1299–1306.

Nurkiewicz, T. R., Porter, D. W., Barger, M., Millecchia, L., Rao, K. M., Marvar, P. J., Hubbs, A. F., Castranova, V., and Boegehold, M. A. (2006). Systemic microvascular dysfunction and inflammation after pulmonary particulate matter exposure. *Environ. Health Perspect.* **114,** 412–419.

Nurkiewicz, T. R., Porter, D. W., Hubbs, A. F., Cumpston, J. L., Chen, B. T., Frazer, D. G., and Castranova, V. (2008). Nanoparticle inhalation augments particle-dependent systemic microvascular dysfunction. *Part Fibre. Toxicol.* **5,** 1.

Oberdorster, G., Sharp, Z., Atudorei, V., Elder, A., Gelein, R., Kreyling, W., and Cox, C. (2004). Translocation of inhaled ultrafine particles to the brain. *Inhal. Toxicol.* **16,** 437–445.

Peretz, A., Sullivan, J. H., Leotta, D. F., Trenga, C. A., Sands, F. N., Allen, J., Carlsten, C., Wilkinson, C. W., Gill, E. A., and Kaufman, J. D. (2008). Diesel exhaust inhalation elicits acute vasoconstriction in vivo. *Environ. Health Perspect.* **116,** 937–942.

Persson, M. G., Gustafsson, L. E., Wiklund, N. P., Hedqvist, P., and Moncada, S. (1990). Endogenous nitric oxide as a modulator of rabbit skeletal muscle microcirculation in vivo. *Br. J. Pharmacol.* **100,** 463–466.

Peters, A., Dockery, D. W., Muller, J. E., and Mittleman, M. A. (2001). Increased particulate air pollution and the triggering of myocardial infarction. *Circulation* **103,** 2810–2815.

Rundell, K. W., Hoffman, J. R., Caviston, R., Bulbulian, R., and Hollenbach, A. M. (2007). Inhalation of ultrafine and fine particulate matter disrupts systemic vascular function. *Inhal. Toxicol.* **19,** 133–140.

Sager, T. M., Kommineni, C., and Castranova, V. (2008). Pulmonary response to intratracheal instillation of ultrafine versus fine titanium dioxide: Role of particle surface area. *Part Fibre. Toxicol.* **5,** 17.

Salom, J. B., Barbery, D., Centeno, J. M., Orti, M., Torregrosa, G., and Alborch, E. (1998). Relaxant effects of sodium nitroprusside and NONOates in rabbit basilar artery. *Pharmacology* **57,** 79–87.

Salom, J. B., Barbery, D., Centeno, J. M., Orti, M., Torregrosa, G., and Alborch, E. (1999). Comparative relaxant effects of the NO donors sodium nitroprusside, DEA/NO and SPER/NO in rabbit carotid arteries. *Gen. Pharmacol.* **32,** 75–79.

Sayes, C. M., Wahi, R., Kurian, P. A., Liu, Y., West, J. L., Ausman, K. D., Warheit, D. B., and Colvin, V. L. (2006). Correlating nanoscale titania structure with toxicity: A cytotoxicity and inflammatory response study with human dermal fibroblasts and human lung epithelial cells. *Toxicol. Sci.* **92,** 174–185.

Schneider, A., Neas, L., Herbst, M. C., Case, M., Williams, R. W., Cascio, W., Hinderliter, A., Holguin, F., Buse, J. B., Dungan, K., Styner, M., *et al.* (2008). Endothelial dysfunction: Associations with exposure to ambient fine particles in diabetic individuals. *Environ. Health Perspect.* **116,** 1666–1674.

Stone, K. C., Mercer, R. R., Gehr, P., Stockstill, B., and Crapo, J. D. (1992). Allometric relationships of cell numbers and size in the mammalian lung. *Am. J. Respir. Cell Mol. Biol.* **6,** 235–243.

Stone, V. F., and Davis, R. J. (1998). Synthesis, characterization, and photocatalytic activity of titania and niobia mesoporous molecular sieves. *Chem. Mater.* **10,** 1468–1474.

Sumimoto, H. (2008). Structure, regulation and evolution of Nox-family NADPH oxidases that produce reactive oxygen species. *FEBS J.* **275,** 3249–3277.

Sun, Q., Yue, P., Ying, Z., Cardounel, A. J., Brook, R. D., Devlin, R., Hwang, J. S., Zweier, J. L., Chen, L. C., and Rajagopalan, S. (2008). Air pollution exposure potentiates hypertension through reactive oxygen species-mediated activation of Rho/ROCK. *Arterioscler. Thromb. Vasc. Biol.* **28,** 1760–1766.

Tamagawa, E., Bai, N., Morimoto, K., Gray, C., Mui, T., Yatera, K., Zhang, X., Xing, L., Li, Y., Laher, I., *et al.* (2008). Particulate matter exposure induces persistent lung inflammation and endothelial dysfunction. *Am. J. Physiol. Lung Cell Mol. Physiol.* **295,** L79–L85.

Tornqvist, H., Mills, N. L., Gonzalez, M., Miller, M. R., Robinson, S. D., Megson, I. L., MacNee, W., Donaldson, K., Soderberg, S., Newby, D. E., *et al.* (2007). Persistent endothelial dysfunction in humans after diesel exhaust inhalation. *Am. J. Respir. Crit. Care Med.* **176,** 395–400.

Urch, B., Silverman, F., Corey, P., Brook, J. R., Lukic, K. Z., Rajagopalan, S., and Brook, R. D. (2005). Acute blood pressure responses in healthy adults during controlled air pollution exposures. *Environ. Health Perspect.* **113,** 1052–1055.

Vasiliev, P. O., Faure, B., Ng, J. B., and Bergstrom, L. (2008). Colloidal aspects relating to direct incorporation of TiO2 nanoparticles into mesoporous spheres by an aerosol-assisted process. *J. Colloid Interface Sci.* **319,** 144–151.

Warheit, D. B. (2008). How meaningful are the results of nanotoxicity studies in the absence of adequate material characterization? *Toxicol. Sci.* **101,** 183–185.

Warheit, D. B., Borm, P. J., Hennes, C., and Lademann, J. (2007). Testing strategies to establish the safety of nanomaterials: Conclusions of an ECETOC workshop. *Inhal. Toxicol.* **19,** 631–643.

Watkinson, W. P., Campen, M. J., Nolan, J. P., and Costa, D. L. (2001). Cardiovascular and systemic responses to inhaled pollutants in rodents: Effects of ozone and particulate matter. *Environ. Health Perspect.* **109**(Suppl. 4), 539–546.

Wellenius, G. A., Saldiva, P. H., Batalha, J. R., Krishna Murthy, G. G., Coull, B. A., Verrier, R. L., and Godleski, J. J. (2002). Electrocardiographic changes during exposure to residual oil fly ash (ROFA) particles in a rat model of myocardial infarction. *Toxicol. Sci.* **66,** 327–335.

Wilcox, C. S. (2003). Redox regulation of the afferent arteriole and tubuloglomerular feedback. *Acta Physiol. Scand.* **179,** 217–223.

Zhang, A. P., and Sun, Y. P. (2004). Photocatalytic killing effect of TiO2 nanoparticles on Ls-174-t human colon carcinoma cells. *World J. Gastroenterol.* **10,** 3191–3193.

Zhang, C., Reiter, C., Eiserich, J. P., Boersma, B., Parks, D. A., Beckman, J. S., Barnes, S., Kirk, M., Baldus, S., Darley-Usmar, V. M., *et al.* (2001). L-arginine chlorination products inhibit endothelial nitric oxide production. *J. Biol. Chem.* **276,** 27159–27165.

Zhang, X. (2004). Real time and in vivo monitoring of nitric oxide by electrochemical sensors—From dream to reality. *Front Biosci.* **9,** 3434–3446.

Zweifach, B. W. (1991). Vascular resistance. In *The Resistance Vasculature* (J. A. Bevan, W. Halpern, M. J. Mulvaney, Eds.), pp. 1–22. Humana Press, Totowa, NJ.